Ionization of Aniline and Its *N*-methyl and *N*-phenyl Substituted Derivatives by (Free) Electron Transfer to *n*-butyl Chloride Parent Radical Cations

Andrej Maroz, Ralf Hermann, Sergej Naumov,† and Ortwin Brede*

University of Leipzig, Interdisciplinary Group Time-Resolved Spectroscopy, Permoserstrasse 15, D-04303 Leipzig, Germany

Received: January 18, 2005; In Final Form: February 18, 2005

The electron transfer from aniline and its *N*-methyl as well as *N*-phenyl substituted derivatives (*N*-methylaniline, *N*,*N*-dimethylaniline, diphenylamine, triphenylamine) to parent solvent radical cations was studied by electron pulse radiolysis in *n*-butyl chloride solution. The ionization results in the case of aniline ($ArNH_2$) and the secondary aromatic amines (Ar_2NH, Ar(Me)NH) in the synchronous and direct formation of amine radical cations, as well as aminyl radicals, in comparable amounts. Subsequently, $ArNH_2^{\bullet+}$ deprotonates in a delayed reaction with the present nucleophile Cl^-, and forms further $ArNH^\bullet$. In contrast, tertiary aromatic amines such as triphenylamine and dimethylaniline yield primarily the corresponding amine radical cations $Ar_3N^{\bullet+}$ or $Ar(Me_2)N^{\bullet+}$, only. The persistent $Ar_3N^{\bullet+}$ forms a charge transfer complex (dimer) with the parent amine molecule, whereas $Ar(Me_2)N^{\bullet+}$ deprotonates to carbon-centered radicals $Ar(Me)NCH_2^\bullet$.

1. Introduction

Aromatic amines are often used in dyestuffs and in antioxidant chemistry.[1,2] Because of the relatively weak N−H bond in the primary and secondary amines ($D_{N-H} = 80-85$ kcal mol^{-1}),[3] these compounds act as H donors in radical reactions. On the other hand, the low ionization potential ($IP_g \approx 7.5$ eV)[3] and the high reduction potential ($E° \approx 1$ V vs normal hydrogen electrode, NHE)[4] results in easy one-electron oxidation of an aromatic amine (i.e., its ionization). These processes have been frequently studied by time-resolved kinetic techniques.

Concerning the bimolecular oxidation of aromatic amines, in aqueous solution the classical one-electron oxidants such as, for example, azide,[4,5] sulfate, and hydroxyl radicals[6−8] generate products of unclear identity: amine radical cations, aminyl radicals, α-*N*-alkyl and cyclohexadienyl-type radicals. This partially holds also for photosensitized electron transfer,[9,10] direct photoionization,[11,12] or electrochemical oxidation.[13]

The main difficulty consists of the identification of the amine transients that mainly results from the very similar optical absorption behavior of the radical cations and the aminyl radicals derived from the aromatic amines. In aqueous solution, the equilibrium pK_a can lead to further complications and errors.

In nonpolar solution, however, the amine transients should be easier to distinguish, at least by time-resolved spectroscopy. In particular, the free electron transfer (FET)[14−16] from the aromatic amines to the parent solvent radical cations derived from alkanes (R−H) and alkyl chlorides (R−Cl) offers a well-defined pathway for the generation of radical cations of aromatic amines. Such solvent radical cations are easy to generate and observe in electron pulse radiolysis, as shown for the case of *n*-butyl choride in reaction 1.

$$n\text{-}C_4H_9Cl \rightsquigarrow n\text{-}C_4H_9Cl^{\bullet+} + e^-_{solv} \quad (1)$$

The ionization electron is immediately scavenged and converted to chloride ions (reaction 2). Then, the diffusion-controlled electron transfer takes place as shown for the example of triphenylamine as donor (reaction 3). This type of FET has

$$e^-_{solv} + n\text{-}C_4H_9Cl \rightarrow n\text{-}\dot{C}_4H_9 + Cl^- \quad (2)$$

$$n\text{-}C_4H_9Cl^{\bullet+} + Ar_3N \rightarrow Ar_3N^{\bullet+} + n\text{-}C_4H_9Cl \quad \text{FET} \quad (3)$$

some peculiarities insofar as after approaching the reactants the real electron jump is a nonhindered and extremely rapid process (proceeding in the sub-femtosecond time range). Hence, this reaction gives access to molecular dynamic effects, even in a bimolecular reaction.[17]

In this paper, we report on the ionization of primary, secondary, and tertiary aromatic amines by free electron transfer. Then, the different decay channels of the amine radical cations are analyzed in detail.

2. Experimental Section

Pulse radiolysis experiments were performed with high-energy electron pulses (1 MeV, 15-ns duration) generated by a pulse transformer accelerator ELIT (Institute of Nuclear Physics, Novosibirsk, Russia). The absorbed dose per pulse measured with an electron dosimeter was between 50 and 100 Gy, corresponding to transient concentrations of around 10^{-5} mol dm^{-3}. Details of the pulse radiolysis setup are reported elsewhere.[18] The solvent *n*-butyl chloride was purified as reported elsewhere.[17] The spectroscopic grade substances from Aldrich and Merck were generally dried using molecular sieve chromatography. The amines were of highest commercial grade (Merck) and used as received. The following amines were used for our study:

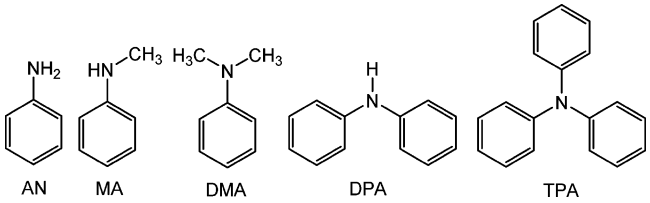

* brede@mpgag.uni-leipzig.de.
† Leibniz Institute of Surface Modification, Permoserstrasse 15, D-04303 Leipzig, Germany.

10.1021/jp0503056 CCC: $30.25
Published on Web 05/07/2005

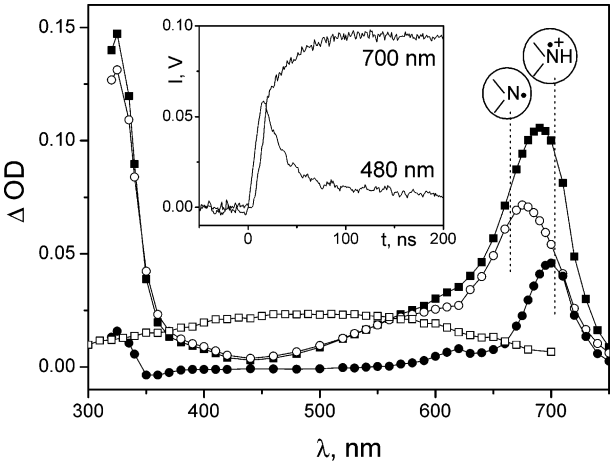

Figure 1. Transient spectrum obtained in the pulse radiolysis of 10^{-3} mol dm^{-3} DPA in deaerated *n*-butyl chloride, taken (■) 40 ns and (○) 1.2 μs after the electron pulse. (●) represents the spectrum of the radical cation of DPA taken as a difference of the above spectra. For comparison, spectrum of the BuCl radical cation is shown (□). Inset: time profiles of the same sample taken at 480 and 700 nm.

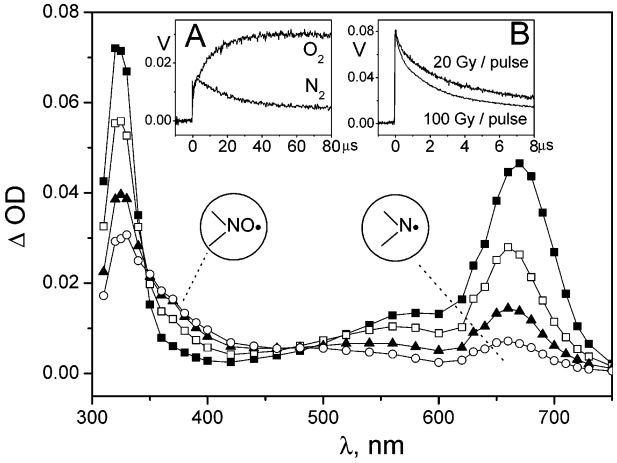

Figure 2. Transient spectrum of an oxygen-saturated 10^{-3} mol dm^{-3} DPA solution in *n*-butyl chloride (■) 1.5 μs, (□) 10 μs, (▲) 33 μs, and (○) 73 μs after the pulse. Inset A: time profiles of deaerated and oxygen-saturated solutions at 380 nm. Inset B: dose-dependent decay at 700 nm.

The kinetic fits of the superimposed transient absorption time profiles were performed using modified versions of the programs ACUCHEM[19] which numerically solve the differential equation for the assumed reaction mechanism. To adjust the concentration profiles to those of optical absorption, reasonable extinction coefficients were used which were determined independently (e.g., by one-electron oxidation in aqueous solution). Quantum chemical calculations were performed with the density functional theory (DFT) hybrid functional B3LYP with the 6-31G(d) basis set using *Gaussian 03*.[20−23] This enabled vibration analysis of the studied molecules and geometry calculation of the frontier orbitals.

3. Results

Pulse Radiolysis of DPA. Because diphenylamine (DPA) represents a prototype of amine antioxidants, this compound has been studied extensively. After pulsing a nitrogen-purged solution of 10^{-3} mol dm^{-3} DPA in *n*-butyl chloride, the primary formed solvent radical cation (480 nm) decays under the concomitant formation of amine transients (around 700 nm). This kinetic correlation can be derived from the time profiles given in the inset in Figure 1.

The rate constant of this electron transfer process is $k = 2 \times 10^{10}$ dm^3 mol^{-1} s^{-1} which is a diffusion-controlled value. The resulting transient optical absorption spectra are given in Figure 1. There are two absorption maxima around $\lambda_{max} = 330$ nm and $\lambda_{max} = 700$ nm. By analyzing the latter absorption at different times, it can be seen that this maximum is caused by two transient absorptions: a short-lived one at $\lambda_{max} = 700$ nm and a longer-lasting absorption with $\lambda_{max} = 670$ nm. This becomes clear by taking the difference spectrum between both transient absorptions. As a tentative interpretation, the transients are assigned to the radical cation $Ar_2NH^{\bullet+}$ ($\tau_{1/2} \approx 500$ ns) and the aminyl radical $Ar_2N^{\bullet}$ ($\tau_{1/2} \approx 10$ μs). The UV absorption is caused by both transients, but in a perfect superimposition, and therefore, kinetic analysis was impossible in this spectral range.

At first glance, oxygen had no marked influence on the observed amine transients. But in the long time range in O_2-saturated solution, the aminyl radical decays under the formation of a stable product ($\lambda_{max} \approx 370$ nm), which is assigned to the nitroxyl radical $Ar_2NO^{\bullet}$, in accordance with reaction 4.[24] These relations can be derived from the time-dependent spectra (cf. Figure 2) where the isosbestic point (∼500 nm) between aminyl decay and nitroxyl formation supports this kinetic interpretation.

$$Ar_2N^{\bullet} + O_2 \rightarrow Ar_2NOO^{\bullet} \quad (4a)$$

$$2Ar_2NOO^{\bullet} \rightarrow 2Ar_2NO^{\bullet} + O_2 \quad (4b)$$

The same facts are reflected in the time profiles taken at 380 and 700 nm (insets in Figure 2). The latter one demonstrates the effect of dose variation on the superimposed signals of $Ar_2NH^{\bullet+}$ and $Ar_2N^{\bullet}$. Even for the short-lived transient, a marked dose influence is observed.

Concerning the ionization of DPA via the described electron transfer, there is evidence for a direct and synchronous formation of amine radical cations as well as aminyl radicals, as symbolized by reaction 5. From the experimental side, this is indicated

$$n\text{-}C_4H_9Cl^{\bullet+} + Ar_2NH \rightarrow n\text{-}C_4H_9Cl + Ar_2NH^{\bullet+}(50\%) + Ar_2N^{\bullet}(50\%) + H^+ \quad (5)$$

in time profiles taken in the spectral range where the aminyl radicals dominate ($\lambda = 500-600$ nm) and, in particular, for higher DPA concentrations where the n-$C_4H_9Cl^{\bullet+}$ spike is reduced into the pulse length. This effect is elucidated in detail in the discussion section.

Concerning the decay of $Ar_2NH^{\bullet+}$, it is observed that these species decay by a reaction with the present nucleophile Cl^- which is formed by the electron reaction 2. Although the diphenylamine radical cations are less reactive, in the presence of Cl^- they become deprotonated according to reaction 6. This

$$Ar_2NH^{\bullet+} + Cl^- \rightarrow Ar_2N^{\bullet} + HCl \qquad k_6 \approx 10^{10}\ \text{dm}^3\ \text{mol}^{-1}\ \text{s}^{-1} \quad (6)$$

reaction represents a time-resolved and therefore delayed channel of aminyl radical formation.

Pulse Radiolysis of Aniline (AN) and Methylaniline (MA). By pulsing millimolar solutions of AN and MA, both substances exhibit a quite similar behavior in electron transfer kinetics and optical absorption spectra of amine radical cations as well as amine radicals.

Figure 3 shows transient optical absorption spectra taken from a solution of 2×10^{-3} mol dm^{-3} solution of AN in *n*-butyl

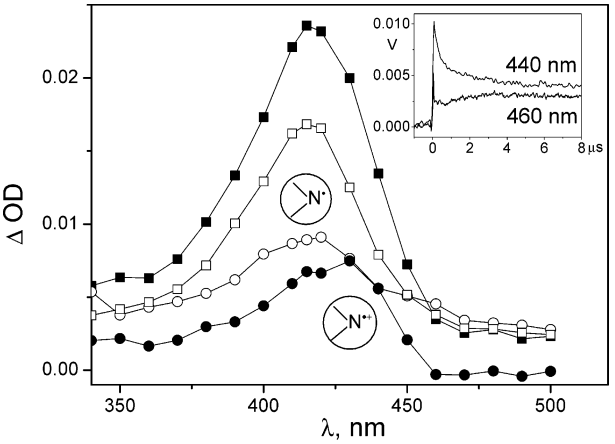

Figure 3. Transient spectrum obtained by pulse radiolysis of 2×10^{-3} mol dm^3 AN in *n*-butyl chloride taken at (■) 50 ns, (□) 500 ns, and (○) 1 μs after the electron pulse. The transient spectrum of the radical cation (●) is given as the difference between the first two spectra. Experimental time profiles are shown as inset.

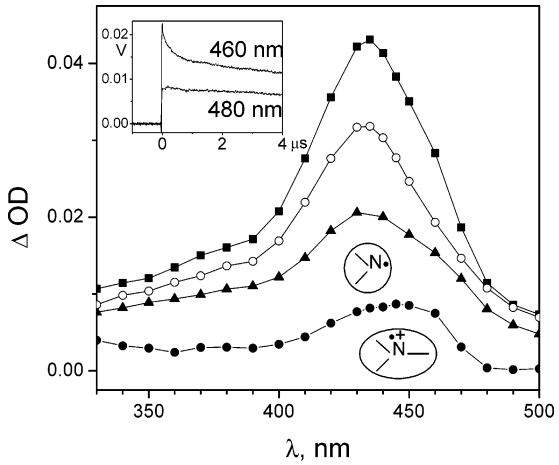

Figure 4. Transient spectra obtained after pulsing a solution of 10^{-2} mol dm^3 MA in *n*-butyl chloride taken (■) 60 ns, (○) 1.9 μs, and (▲) 10 μs after the pulse. The transient spectrum of the MA radical cation (●) was obtained as the difference between spectra taken at short times (60 and 800 ns). Experimental time profiles are shown as inset.

chloride at different times after the pulse. The absorption band around 420 nm is caused by a strong superimposition of two different transients, a short-lived one and a long-lasting one. As products of the electron transfer (reaction 5), the species are assigned to be the amine radical cation ($\lambda_{max} = 430$ nm) and the aminyl radical ($\lambda_{max} = 415$ nm). The distinction of the species can be realized by taking the difference spectrum at short times and by analyzing the time profiles at convenient wavelengths, as shown in Figure 3 and the corresponding inset. After observation of the time profiles, it should be mentioned that the spike in the very beginning is caused by the residual absorption of *n*-$C_4H_9Cl^{\bullet+}$.

Figure 4 shows the analogous situation for a pulsed solution of 10^{-2} mol dm^{-3} of MA in *n*-C_4H_9Cl. Here, the amine radical cation peaks around $\lambda_{max} = 445$ nm, whereas the aminyl radicals have a maximum between 430 and 435 nm. From the asymmetrical shape of the spectra, however, the identification of two species is justified. This is also supported by looking at the time profiles given as insets of Figure 4. The spike at 460 nm is caused by the amine radical cation. An analysis of expected UV bands of MA transients was impossible because of the high self-absorption of MA under pulse radiolysis conditions. The immediate formation of the long-lasting absorption can be explained only partially by a superimposition of both MA transients where the radical cation subsequently forms the aminyl radical.

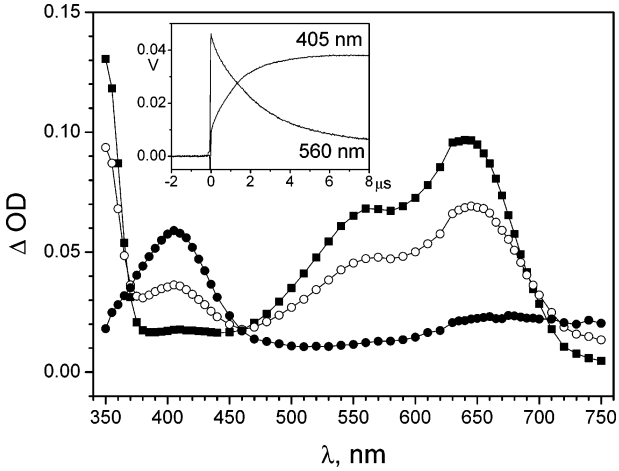

Figure 5. Transient spectra obtained in the pulse radiolysis of a deaerated solution of 5×10^{-3} mol dm^{-3} TPA in *n*-butyl chloride taken (■) 200 ns, (○) 1 μs, and (●) 6.3 μs after the electron pulse. Experimental time profiles are shown as inset.

As already mentioned for DPA, in the cases of AN and MA, a rapid formation of amine radical cations as well as of aminyl radicals as a direct consequence of the electron transfer is also observed, quite analogous to reaction 4.

Ionization of the Tertiary Amines Triphenylamine (TPA) and Dimethylamine (DMA). Ionization of the tertiary amines TPA and DMA should result in persistent amine radical cations.[25,26] Indeed, by pulsing a solution of 5×10^{-3} mol dm^{-3} TPA in *n*-butyl chloride, the spectra given in Figure 5 are obtained.

The direct product of the electron transfer (reaction 3) is the amine radical cation which shows the well-known spectra[27] with $\lambda_{max} = <350$, 570, and 640 nm. Dependent on the parent amine concentration, the (monomer) amine cations decay under the formation of a dimer radical cation ($\lambda_{max} = 405$ nm) which in reality represents a charge transfer complex analogous to many other arene radical cationic systems[28,29] (see inset in Figure 5 and reaction 7). Because of the equilibrium situation (reaction 7) and the competing neutralization (reaction 8), the rate constant k_7 is estimated only.

$$Ar_3N^{\bullet+} + Ar_3N \rightleftharpoons (Ar_3N)_2^{\bullet+} \quad k_7 \approx 7 \times 10^7 \text{ dm}^3 \text{ mol}^{-1} \text{ s}^{-1} \tag{7}$$

$$Ar_3N^{\bullet+} + Cl^- \rightarrow \text{products} \tag{8}$$

The electron transfer ionization of DMA yielded the corresponding amine radical cation as the only direct product. These species exhibit optical absorption spectra peaking at $\lambda_{max} = 470$ nm (cf. Figure 6).

There is no indication of a further direct product of the electron transfer as observed in the case of aniline and the secondary aromatic amines. In distinction to TPA, no dimerization (like that shown by reaction 7) could be seen. Instead, the cations $DMA^{\bullet+}$ decay by reaction with the counter charge, that is, with the chloride ion. The product is an alkyl radical

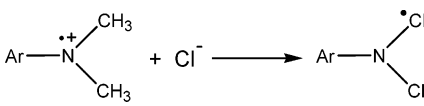

(9)

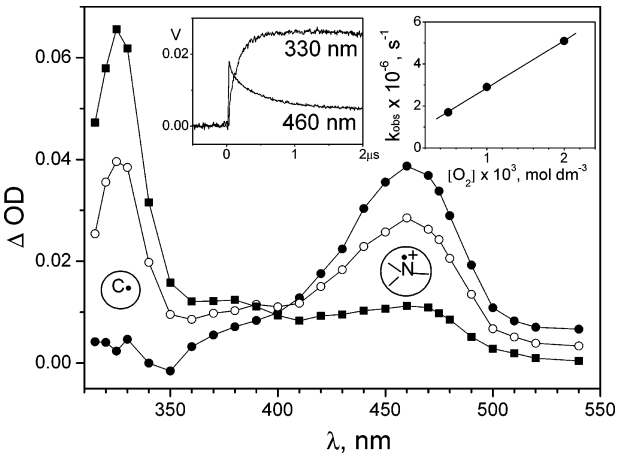

Figure 6. Transient spectra obtained in the pulse radiolysis of 5×10^{-3} mol dm^{-3} DMA in *n*-butyl chloride purged with N_2, taken (●) 30 ns, (○) 140 ns, and (■) 1.7 μs after the pulse. Insets: experimental time on the left. Stern−Volmer plot for the quenching of C• with oxygen analyzed at 330 nm (right side).

formed by deprotonation at one of the methyl groups; see reaction 9. Such reactions were already observed for tertiary aliphatic amine radical cations[30] and supported in our paper by the variation of the dose per pulse.

The α-aminoalkyl radical can be identified kinetically by the observation of the isosbestic point at 400 nm between the decay of the Ar−N−$Me_2^{\bullet+}$ absorption and the alkyl radical formation. As expected, the alkyl radical reacts with oxygen according to reaction 10, and therefore, its absorption is efficiently quenched. This is demonstrated by the Stern−Volmer plot given as the inset in Figure 6.

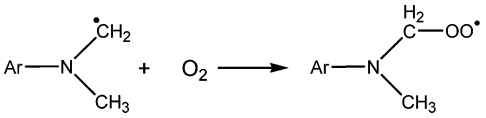

(10)

$$k_{10} = 2 \times 10^9 \text{ dm}^3 \text{ mol}^{-1} \text{ s}^{-1}$$

4. Discussion

Principles of Free Electron Transfer. Electron transfer in nonpolar systems exhibits some peculiarities.[14−17] In the widest sense, it stands between the phenomena of gas-phase and liquid-phase kinetics. The participating ions are only very weakly solvated. Hence, collisions of the reaction partners could be understood more as hard-core interactions and result either in an immediate reaction or in elastic repulsion. On the other side, the surrounding solvent causes a rapid relaxation of excess energy, and therefore, in comparison with gas-phase conditions, it results in a higher stability of metastable transients such as, for example, σ-type solvent radical cations of alkanes and alkyl chlorides.

The electron transfer of the type in reaction 3 proceeds with thermalized solvent ions in a rapid and diffusion-controlled manner. After splitting the process into single steps, the diffusional approach of the reactants is the rate-determining step. The collision of the reactants is combined with the electron jump or, otherwise, with elastic renewed separation of the participating molecules. This seems to be a peculiarity of FET in nonpolar systems, that is, reaction in the first approach without any longer interaction interval as, for example, the encounter complex in the classical electron transfer understanding.[31,32] In the course of collision, the electron jump itself is an extremely rapid and

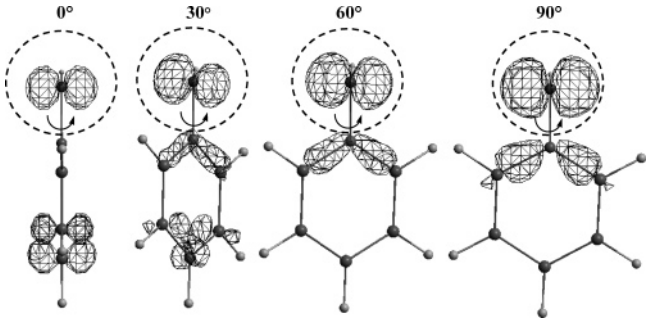

Figure 7. Transformation of n-orbital of the Ar−OH singlet ground state (isocontur = 0.1) in dependence on OH-group rotation.

nonhindered process comparable with the electron flux in aromatic rings. This is suggested to happen in a time range of hundreds of attoseconds up to the femtosecond border. So, the electron jump is much faster than any vibration or bending motions within the molecules.

From other donor systems (phenols,[14,17] thiophenols,[33] benzylsilanes,[15] etc.) it is known that the femtosecond electron jump identifies different momentary conformer situations of the donor molecule which are conditioned by the bending motions of substituents of the molecule. That is the case if the molecular bending motions are accompanied by marked electron shifts. This phenomenon is illustrated in the reaction sequence in Scheme 1 on the example of phenol (ArOH) as donor: In

SCHEME 1

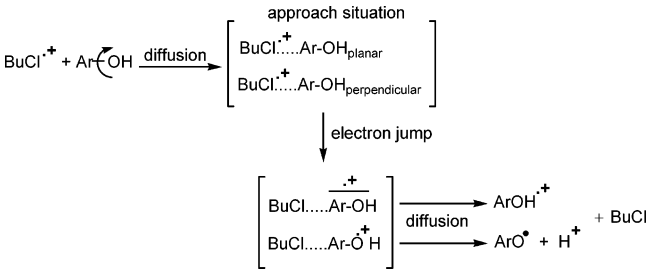

phenol, the C−OH bending motion (rotation) has a frequency of about 10^{13} Hz. So, in the time range of 10^{-13} s, the n-electrons of the oxygen atom fluctuate between a planar and perpendicular molecule conformer structure. During this motion, all of the conformer situations are attained and passed through. This is illustrated by a quantum chemical calculation of the electron distribution for different angles of bending; see Figure 7.

But by reason of kinetic analysis, only the borderline cases (planar or perpendicular) are considered. In the planar case (0° twist), the n-electrons are distributed over the whole molecule, whereas in the perpendicular structure (90° twist), the electrons are localized mainly at the heteroatom. In the reaction sequence in Scheme 1, both borderline situations of the reactants are temporarily realized. They are visualized in the structures of the resulting cations (in brackets).

It is obvious that the planar radical cation structure overcomes, whereas the species with an electron localized at oxygen deprotonates rapidly, assisted by the solvent. The different conformer structures can be identified by the two immediately formed products such as the radical cation and the phenoxyl radical.

FET Involving Aniline and Secondary Aromatic Amines. As demonstrated in the preceding section, a similar effect was also observed for the FET involving aromatic amines, in particular, in the cases of the primary and secondary amines such as aniline, methylaniline, and diphenylamine. Derived from

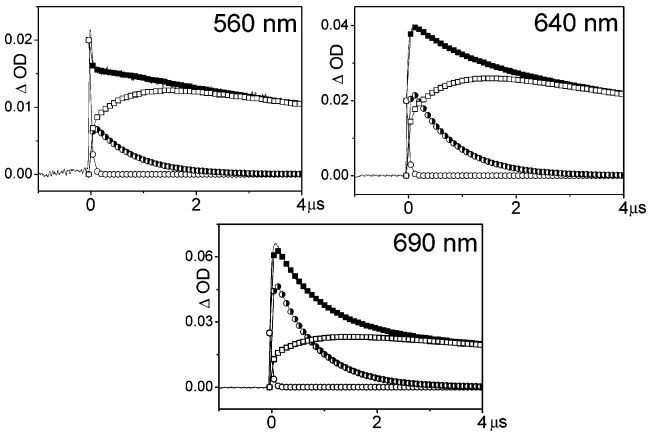

Figure 8. Time profiles showing the correlation between kinetic simulation and experimental data: (−) experimental profile, (■) simulated time profile, (○) chlorobutane radical cation, (◑) DPA radical cation, (□) DPA radical.

SCHEME 2

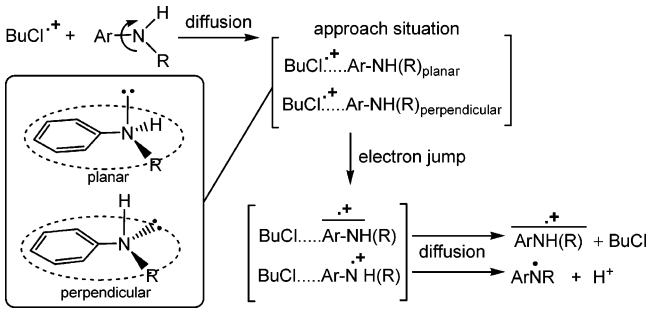

the analysis of the decay of the solvent parent ion (n-C_4H_9-$Cl^{\bullet+}$) in the presence of the amines, the overall electron transfer (reaction 3) proceeds with a diffusion-controlled rate constant $k_3 \approx 10^{10}$ dm^3 mol^{-1} s^{-1}. On the product side, however, a more complex behavior appears. This is now described for the case of DPA. As already mentioned in the preceding section, DPA$^{\bullet+}$ and DPA$^{\bullet}$ are formed as direct products of the electron transfer (reaction 5).

The time-dependent spectra of the transients (Figure 1) give strong evidence for this. However, the situation becomes much more clear by analyzing time profiles at different characteristic wavelengths (see Figure 8). The experimental profiles taken at 560, 640, and 690 nm differ in shape and result mainly from superpositions of different parts of a short-living (DPA$^{\bullet+}$) and a long-lasting (DPA$^{\bullet}$) transient. The time profiles were simulated by using the electron transfer (equation 5) as a rapid generation function for the promptly formed transients DPA$^{\bullet+}$ and DPA$^{\bullet}$ and by describing the delayed decay of DPA$^{\bullet+}$ with the deprotonation reaction 6.

On the basis of this, all three time profiles could be described numerically by fixed kinetic parameters. From the relation between the rapid (prompt) and the delayed part of the DPA$^{\bullet}$ absorption, the ratio between both channels of the electron transfer (Scheme 2) can be estimated to be about 50:50. This is derived from the time profiles of the aminyl radicals of DPA. Each profile consists of a rapid part and a delayed part of the same ratio. So, we could calculate this ratio without the knowledge of extinction coefficients, which are difficult to determine under the conditions of nonpolar media. For AN and MA, similar effects were observed which could be treated only qualitatively because of less clear spectral separations. But in general, an explanation of the FET behavior of DPA, AN, and MA in analogy to the phenol systems seems to be justified.

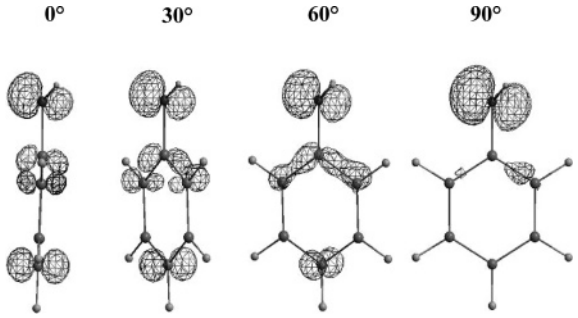

Figure 9. Transformation of HOMO of the Ar−NH_2 (−5.39, −5.47, −5.82, and −6.31 eV) singlet ground state (isocontur = 0.1) in dependence on NH_2-group rotation.

For the aromatic amines, the bending motion center is the amine nitrogen which carries three bonds and a lone electron pair according to the sp^3 hybridization. For the simplest case of aniline, the quantum chemical analysis of the electron shift concomitant with the angle of the bending motion is shown in Figure 9, where the amine group is fixed and the aromatic ring is allowed to twist. It is obvious that in the planar state (0°) the electron distribution happens over the whole molecule, whereas in the other extreme (90°), the HOMO electrons are fully localized at the nitrogen atom.

For diphenylamine also, bending motions around the N−Ar bonds exist. Because of the substitution with two benzene rings, it is a coupled motion in the opposite directions, as indicated in Scheme 2.

Nevertheless, the description of the motion of the rings can be made by quantum chemical calculation of the bending, assuming fixed angles. So, Figure 10 shows the electron distribution in the planar (which is not really the most stable conformer) and perpendicular states. Here also, distribution of the electron density as well as localization can be well-distinguished. Certainly, we have to consider that the bending is a dynamic behavior, and therefore, all imaginable twisting angles and twisting conformers exist at the same time (i.e., in a broad distribution). The distinction of the two borderline states represents an extreme simplification, but may help to understand the processes.

Now, it is assumed that the electron jump from the amines to the solvent radical identifies the conformer situation in the momentum of the electron transfer. In analogy to the already mentioned example of the phenols,[14,17] a metastable and an unstable radical cation should be generated. Because of the resulting local charge at nitrogen, the latter one deprotonates immediately, assisted by the solvent. Then, as practically direct products of the electron transfer, comparable amounts of amine radical cations and of aminyl radicals are formed, which is in good accordance with the experimental behavior discussed above. The phenomenon is observed for AN, MA, and DPA (i.e., for all studied nontertiary amines) and will be illustrated for the case of a substituted aniline (R = Ar, Me) as electron donor; see the reaction sequence in Scheme 2.

Semiquantitative Interpretation of FET Involving Aromatic Amines with DFT Calculations. The electron distribution of the HOMO of the aromatic amines in the ground state was calculated by means of the DFT method. The variation of the molecule geometry and, in particular, the change of the angle of twist of the bonds from nitrogen to carbon of alkyl or aryl

C -↻- NH -↻- C

substituents resulted in a change of the electron density distribution from being smeared over the whole molecule to

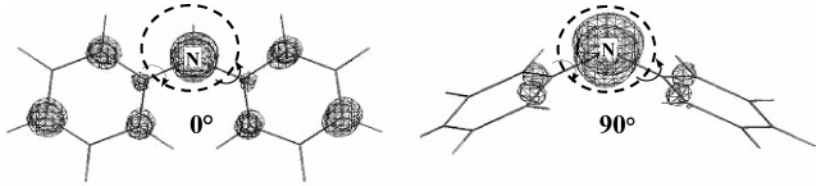

Figure 10. Electron distribution of the HOMO electrons of DPA given for planar state (0°) and twisted state (90°).

TABLE 1: DFT B3LYP/6-31G(d) Calculated Quantum Chemical Data: Frequencies (scale factor $f = 0.96$) of Polar NH-Group Rotation and Valence N−H Vibration Oscillations[a]

solute	ν_{rot} (cm^{-1})	t_{rot} (10^{-15} s)	ν_{oscil} (cm^{-1})	t_{oscil} (10^{-15} s)	IP_{gas} (eV)
Ph−NH_2	564	59.1	3648	9.14	7.2
Ph−NH−CH_3	99.9	334	3596	9.28	7.0
Ph−NH−Ph	54.9	608	3614	9.23	6.7
Ph−$N(CH_3)_2$					6.8
Ph_3N					6.35

[a] t = times of one motion; IP_{gas} = calculated gas-phase ionization potential.

localization at the nitrogen atom, as shown in Figures 9 and 10. Furthermore, the dynamics of the bending motion of the bonds and also the vibration of the >N−H bond has been calculated. The data are given in Table 1. The vibrations have a frequency around 10^{14} Hz for all studied amines, and the rotation motions (bending) happen with frequencies in the range $(2-20) \times 10^{13}$ Hz (i.e., they are much slower as vibrations).

So, in the cases of aniline and the secondary aromatic amines, we state that the described extremely rapid electron jump can identify all states of bending motion around the −NH− group, resulting in two types of radical cations. The stable amine radical cation is that with delocalized spin distribution, whereas that with the spin localized at the nitrogen atom decays immediately by deprotonation. This process is favored from kinetic (oscillation of the N−H bond) and energetic reasons, because the ground level of both states (plane and perpendicular) differs by about 37 kcal mol^{-1}. Then, the proton affinity of the solvent becomes comparable to or larger than that of the amine radical, which certainly assists the deprotonation.

Energetics of the Deprotonation of the Amine Radical Cations. Radical cations derived from aromatic amines are relatively stable species. Radical cations of tertiary aromatic amines are practically persistent.[34] In the presence of a strong nucleophile, however, these radical cations tend to deprotonate. Hence, in this paper, the deprotonation of all studied amine radical cations is apparent in the presence of the counter charge chloride (cf. reactions 6 and 9). These deprotonations are bimolecular processes taking place with diffusion-controlled rate constants $k \approx 10^{10}$ dm^3 mol^{-1} s^{-1}. But because of the great excess of Cl^-, the reaction appears kinetically as a pseudo-first-order process; see the time profiles in Figure 2 inset B.

The monomolecular deprotonation of the radical cations of the aromatic amines, however, is assumed to proceed only in the perpendicular state of the species (see explanations given above). If the ground-state molecule is ionized, the critical C−N bond becomes more rigid. Hence, the activation energy of the bond rotation increases considerably. This means that in the ionized state any bending motion is nearly improbable. Then, it is worth analyzing the energetics of the deprotonation of the twisted (perpendicular) radical ions. Calculations show that, in comparison with the stable planar species, the proton affinity of the perpendicular cation drops by about 37 kcal mol^{-1}. This is enough to remain under the proton affinity of the solvent,

TABLE 2: Transient Absorption Characteristics for the Substances Studied[a]

substance	λ_{max} ($N^{\bullet+}$) nm	ϵ ($N^{\bullet+}$) dm^3 mol^{-1} cm^{-1}	λ_{max} ($N^{\bullet}$) nm	ϵ ($N^{\bullet}$) dm^3 mol^{-1} cm^{-1}
AN	430	$_{406}3300^{5}$ $_{423}4100^{5}$ $_{430}2000^{34}$	415	$_{405}1250^{5}$ $_{400}670^{34}$
MA	450	$_{460}\sim2400^{35\,a}$	430	$_{420}\sim2000^{35\,a}$
DMA	460	$_{480}4500^{36}$	325[b] (Ph−N−C$^{\bullet}$$H_2$)	
DPA	<330 700	$_{315}7600^{6}$ $_{670}18000^{6}$ $_{320}15000^{8}$ $_{700}1200^{8}$ $_{670}27000^{37}$	325 660	$_{315}10000^{6}$ $_{670}2200^{6}$ $_{335}13000^{8}$ $_{675}8000^{8}$
TPA	560 640	$_{650}29000^{38}$		

[a] Wavelengths for literature data are given as a subscripts. [b] Values for *N*-phenylglycine. [c] Absorption maximum for the corresponding α-carbon-centered radical.

and therefore, an immediate and very rapid deprotonation can happen. For our rapid deprotonation of the amine radical cations in the perpendicular state, the deprotonation can be treated as a solvent-assisted process. That means that the solvent is involved in the deprotonation by stabilizing the free proton (reaction 11).

$$Ar_2N-H_{perp.}^{\bullet+} + n\text{-}C_4H_9Cl \rightarrow Ar_2N^{\bullet} + H^+(n\text{-}C_4H_9Cl) \quad (11)$$

Electron Transfer with Tertiary Aromatic Amines. As already mentioned, in the case of TPA and DMA in the electron transfer to solvent radical cations, only one direct product transient is formed, the amine radical cation. This can be understood because of the energetic situation in which the N−C bonds do not dissociate easily because of the unfavorable energetics of the resulting methyl or phenyl cations. However, the decay behavior of the radical cations is very different. The stable $TPA^{\bullet+}$ dimerizes according to the equilibrium (reaction 7), and finally, it decays by neutralization. $DMA^{\bullet+}$, however, gets deprotonated by reaction with the nucleophile (reaction 9). The resulting C-centered radicals could be well-characterized by the oxygen reaction 10.

Survey about Spectral Properties of the Amines. The interpretations given in this paper are based on a very thorough analysis of the spectra of the radical cations and aminyl radicals derived from the aromatic amines, which are strongly superimposed and differ in their absorption maxima in most cases by only 10−20 nm. Table 2 gives absorption maxima taken from our own measurements in comparison to literature data. Furthermore, extinction coefficients are given which were found in the literature. Such values could not be derived from our own measurements because of difficulties in the exact determination of the free ion yield.

5. Conclusions

The processes investigated in this paper are summarized in conclusion in the reaction in Scheme 3. Here, the observed

SCHEME 3

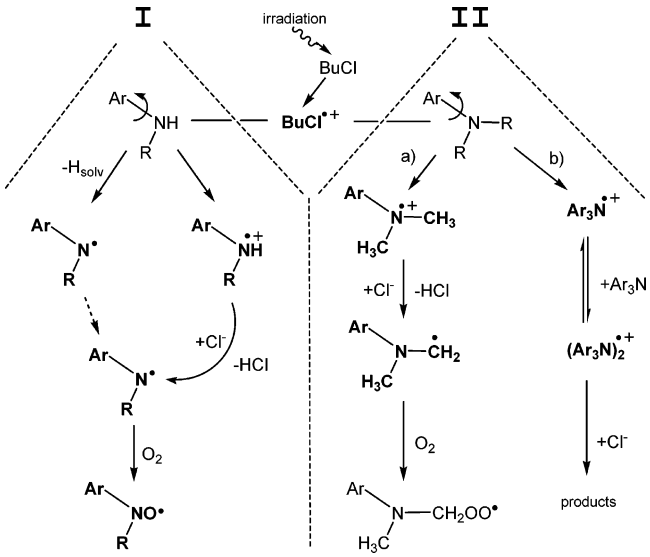

products are marked by boldface type. The reaction mechanism might be distinguished by two lines, with primary and secondary amines in line I and tertiary amines in line II.

The free electron transfer from aromatic amines to solvent radical cations under nonpolar conditions results in the formation of amine radical cations. This statement holds in an unrestricted manner for the studied tertiary amines such as dimethylaniline and triphenylamine.

In the case of aniline and the secondary amines MA and DPA, however, the direct FET products consist of a mixture of amine radical cations and aminyl radicals which appear in nearly equal amounts (see line I in Scheme 3). This phenomenon is explained by an effect of molecular dynamics where the molecular oscillations of the amines (bending) in the ground state lead to a permanently existing mixture of conformers, differing from each other by the angle of rotation (bending). In fact, the rotation-conditioned conformers differ by a different electron density distribution, which is directly caused by the motion. This is indicated by the rotating arrows in the amine ground state (see Scheme 3). In the nonpolar system, the extremely rapid electron jump from the donor molecule (conformer mixture) to the solvent radical cation enables the identification of the different conformers in such cases where the products of the electron transfer are different (stable and unstable amine radical cations). To understand this situation in a very simplified manner, the conformer mixtures are described by two borderline structures such as planar and perpendicular rotation states (see also Scheme 2). The monomolecular deprotonation of the perpendicular radical cation is assisted by the solvent indicated by the state of the proton.

Dependent on the amine structure, the primary ionization products have a different fate, which is indicated by the subsequent reactions given in Scheme 3.

References and Notes

(1) Scott, G. *Atmospheric Oxidation and Antioxidants*; Elsevier: Amsterdam, 1993; Vols. I, II.

(2) Schnabel, W. *Polymer Degradation*; Hanser: Munich, 1992.

(3) Wedenejev, W. J.; Gurwitsch, L. W.; Kondratjew, W. H.; Medwedew, W. A.; Frankewitscch, E. L. *Energien chemischer Bindungen, Ionisationspotentiale und Elektronenaffinitäten*; VEB Verlag für die Grundstoffindustrie: Leipzig, 1971.

(4) Jonsson, M.; Lind, J.; Eriksen T. E.; Merenyi, G. *J. Am. Chem. Soc.* **1994**, *116*, 1423.

(5) Qin, L.; Tripathi, G. N. R.; Schuler, R. H. *Z. Naturforsch.* **1985**, *40a*, 1026.

(6) Schmidt, K. H.; Bromberg, A.; Meisel, D. *J. Phys. Chem.* **1985**, *89*, 4352.

(7) Singh, T. S.; Gejji, S. P.; Rao, B. S. M.; Mohan, H.; Mittal J. P. *J. Chem. Soc., Perkin Trans. 2* **2001**, *7*, 1205.

(8) Rao, B. S. M.; Hayon, E. *J. Phys. Chem.* **1975**, *79*, 1063.

(9) (a) Sandanayaka, A. S. D.; Sasabe, H.; Araki, Y.; Furusho, Y.; Ito, O.; Takata, T. *J. Phys. Chem. A* **2004**, *108* (24), 5145. (b) Kumbhakar, M.; Nath, S.; Pal, H. *J. Chem. Phys.* **2003**, *119* (1), 388.

(10) Rath, M. C.; Pal, H.; Mukherjee, T. *J. Phys. Chem. A* **1999**, *103* (26), 4993.

(11) Ogawa, T.; Ogawa, T.; Nakashima, K. *J. Phys. Chem. A* **1998**, *102*, 10608.

(12) Saito, F.; Tobita, S.; Shizuka, H. *J. Photochem. Photobiol., A: Chem.* **1997**, *106*, 119.

(13) Oyama, M.; Kambayashi, M. *Electrochem. Commun.* **2002**, *4*, 759.

(14) Brede, O.; Hermann, R.; Naumann, W.; Naumov, S. *J. Phys. Chem. A* **2002**, *106*, 757.

(15) Brede, O.; Hermann, R.; Naumov, S.; Perdikomatis, G. P.; Zarkadis, A. K.; Siskos, M. G. *Phys. Chem. Chem. Phys.* **2004**, *6*, 2267.

(16) Brede, O.; Naumov, S.; Hermann, R. *Radiat. Phys. Chem.* **2003**, *67*, 225.

(17) Brede, O.; Hermann, R.; Karakostas, N.; Naumov, S. *Phys. Chem. Chem. Phys.* **2004**, *6*, 5184.

(18) Brede, O.; David, F.; Steenken, S. *J. Chem. Soc., Perkin Trans.* **1995**, *2*, 23.

(19) Braun, W.; Herron, J. T.; Kahaner, D. K. *Int. J. Chem. Kinet.* **1988**, *20*, 51.

(20) Frisch, M. J.; Trucks, G. W.; Schlegel, H. B.; Scuseria, G. E.; Robb, M. A.; Cheeseman, J. R.; Montgomery, Jr., J. A.; Vreven, T.; Kudin, K. N.; Burant, J. C.; Millam, J. M.; Iyengar, S. S.; Tomasi, J.; Barone, V.; Mennucci, B.; Cossi, M.; Scalmani, G.; Rega, N.; Petersson, G. A.; Nakatsuji, H.; Hada, M.; Ehara, M.; Toyota, K.; Fukuda, R.; Hasegawa, J.; Ishida, M.; Nakajima, T.; Honda, Y.; Kitao, O.; Nakai, H.; Klene, M.; Li, X.; Knox, J. E.; Hratchian, H. P.; Cross, J. B.; Bakken, V.; Adamo, C.; Jaramillo, J.; Gomperts, R.; Stratmann, R. E.; Yazyev, O.; Austin, A. J.; Cammi, R.; Pomelli, C.; Ochterski, J. W.; Ayala, P. Y.; Morokuma, K.; Voth, G. A.; Salvador, P.; Dannenberg, J. J.; Zakrzewski, V. G.; Dapprich, S.; Daniels, A. D.; Strain, M. C.; Farkas, O.; Malick, D. K.; Rabuck, A. D.; Raghavachari, K.; Foresman, J. B.; Ortiz, J. V.; Cui, Q.; Baboul, A. G.; Clifford, S.; Cioslowski, J.; Stefanov, B. B.; Liu, G.; Liashenko, A.; Piskorz, P.; Komaromi, I.; Martin, R. L.; Fox, D. J.; Keith, T.; Al-Laham, M. A.; Peng, C. Y.; Nanayakkara, A.; Challacombe, M.; Gill, P. M. W.; Johnson, B.; Chen, W.; Wong, M. W.; Gonzalez, C.; Pople, J. A. *Gaussian 03*, Revision A.1; Gaussian, Inc., Wallingford CT, 2004.

(21) Becke, A. D. *J. Chem. Phys.* **1993**, *98*, 5648.

(22) Becke, A. D. *J. Chem. Phys.* **1996**, *104*, 1040.

(23) Lee, Ch.; Yang, W.; Parr, R. G. *Phys. Rev. B* **1987**, *37*, 785.

(24) Ingold, K. U. In *Landolt Börnstein − Group II Molecules and Radicals*; Springer-Verlag: Heidelberg, 1994; Vol. 18(C), p 251.

(25) Shida, T. *Electronic Absorption Spectra of Radical Ions*; Elsevier: Amsterdam, 1988.

(26) Zador, E.; Warman, J. M.; Hummel, A. *J. Chem. Soc., Faraday Trans. 1* **1976**, *72*, 1368.

(27) Lomoth, R.; Brede, O. *Chem. Phys. Lett.* **1998**, *288*, 47.

(28) Rodgers, M. A. J. *J. Chem. Soc., Faraday Trans. 1* **1972**, *68*, 1278.

(29) Egusa, S.; Tabata, Y.; Arai, S.; Kira, A.; Imamura, M. *Radiat. Phys. Chem.* **1977**, *9*, 419.

(30) Brede, O.; Beckert, D.; Windolph, C.; Göttinger, H. A. *J. Phys. Chem. A* **1988**, *102*, 1457.

(31) Rehm, D.; Weller, A. *Ber. Bunsen-Ges. Phys. Chem.* **1969**, *73*, 834.

(32) Kavarnos, G. V. *Fundamentals of Photoinduced Electron Transfer*; VCH: Weinheim, 1993.

(33) Hermann, R.; Dey, G. R.; Naumov, S.; Brede, O. *Phys. Chem. Chem. Phys.* **2000**, *2*, 1213.

(34) Land, E. J.; Porter, G. *Trans. Faraday Soc.* **1963**, *59*, 2027.

(35) Canle, M.; Santaballa, J. A.; Steenken, S. *Chem.—Eur. J.* **1999**, *5* (4), 1192.

(36) Poizat, V. O.; Guichard, G.; Buntinx, K. D. *J. Phys. Chem.* **1989**, *90*, 4697.

(37) Johnston, L. J.; Redmond, R. W. *J. Phys. Chem.* **1997**, *101*, 4660.

(38) Burrows, H. D.; Graetorex, D.; Kemp, T. J. *J. Phys. Chem.* **1972**, *76*, 20.